J|A|C|S
ARTICLES
Published on Web 12/08/2005

Direct-Detected ^{13}C NMR to Investigate the Iron(III) Hemophore HasA

Célia Caillet-Saguy,[†] Muriel Delepierre,[†] Anne Lecroisey,*[,†] Ivano Bertini,[‡] Mario Piccioli,[‡] and Paola Turano[‡]

Contribution from the Unité de RMN des Biomolécules (CNRS URA 2185), Institut Pasteur, Paris, France, and CERM and Department of Chemistry, University of Florence, Sesto Fiorentino, Florence, Italy

Received July 21, 2005; E-mail: alecrois@pasteur.fr

Abstract: Hemophore HasA is a 19 kDa iron(III) hemoprotein that participates in the shuttling of heme to a specific membrane receptor. In HasA, heme iron has an original coordination environment with a His/Tyr pair as axial ligands. Recently developed two-dimensional protonless ^{13}C-detected experiments provide the sequence-specific assignment of all but three protein residues in the close proximity of the paramagnetic center, thus overcoming limitations due to the short relaxation times induced by the presence of the iron(III) center. Mono-dimensional ^{13}C and ^{15}N experiments tailored for the detection of paramagnetic signals allow the identification of resonances of the axial ligands. These experiments are used to characterize the conformational features and the electronic structure of the heme iron(III) environment. The good complementarity among ^{1}H-, ^{13}C-, and ^{15}N-detected experiments is highlighted. A thermal high-spin/low-spin equilibrium is observed and is related to a modulation of the strength of the coordination bond between the iron and the Tyr74 axial ligand. The key role of a neighboring residue, His82, for the stability of the axial coordination and its involvement in the heme delivery to the receptor is discussed.

Introduction

Paramagnetic NMR spectroscopy has the power to provide information on both the structural properties and the electronic structure of the active sites of paramagnetic metalloproteins.[1,2] However, exploitation of this synergism is often hampered by paramagnetic relaxation that causes broadening, even beyond detection, of signals of nuclei in the vicinity of the metal ion. This effect is modulated by the electron relaxation time, which in turn depends on the type of metal ion, on the coordination geometry,[3] and on the size of the molecule. Within this frame, the case of highly paramagnetic iron(III) within heme proteins represents one of the most challenging cases.

The ^{13}C route allows the investigation of high molecular weight proteins[4−6] as well as paramagnetic proteins.[7−10] Paramagnetic relaxation depends on the square of the gyromagnetic ratio γ of the investigated nucleus; when passing from ^{1}H to ^{13}C detection, the dipolar contribution to relaxation rates of the observed signals decreases by roughly a factor of 16 ($\gamma_H = 2.67 \times 10^{-8}$ rad s^{-1} T^{-1}; $\gamma_C = 6.73 \times 10^{-7}$ rad s^{-1} T^{-1}). Therefore, the availability of NMR experiments that rely on ^{13}C direct detection allows us to decrease signal losses due to fast nuclear relaxation.[11] The efficiency of this approach, which has been proven successful for copper(II) proteins[12,13] and lanthanide-substituted calcium binding proteins,[14] relies on the ability to overcome the splitting due to $^{13}C-^{13}C$ scalar coupling.[6] Here, we use ^{13}C direct detection to approach a highly paramagnetic iron(III) heme protein, as ^{1}H NMR proved to be of limited use. We perform an extensive assignment of the protein, even in the very close environment of the iron(III) paramagnetic center, not only to learn about the structure but also to probe the conformational equilibrium experienced by the system.

The protein HasA belongs to the hemophores, which are small extracellular proteins that form an independent family of heme-binding proteins with no homology to any known proteins. They are secreted under iron-limiting conditions by an ABC trans-

* To whom correspondence should be addressed. Institut Pasteur, 28 rue du Docteur Roux, 75015 Paris cedex 05, France. Phone: 01 40 61 36 67. Fax: 01 45 68 89 29.
[†] Institut Pasteur.
[‡] University of Florence.

(1) Bertini, I.; Turano, P.; Vila, A. J. *Chem. Rev.* **1993**, *93*, 2833−2932.
(2) Bertini, I.; Luchinat, C.; Piccioli, M. *Methods Enzymol.* **2001**, *339*, 314−340.
(3) Bertini, I.; Luchinat, C.; Parigi, G. *Elsevier* **2001**.
(4) Oh, B. H.; Westler, W. M.; Darba, P.; Markley, J. L. *Science* **1988**, *240*, 908−911.
(5) Hu, K.; Eletsky, A.; Pervushin, K. *J. Biomol. NMR* **2003**, *26*, 69−77.
(6) Bermel, W.; Bertini, I.; Duma, L.; Felli, I. C.; Emsley, L.; Pierattelli, R.; Vasos, P. R. *Angew Chem., Int. Ed. Engl.* **2005**, *44*, 3089−3092.
(7) Bertini, I.; Lee, Y. M.; Luchinat, C.; Piccioli, M.; Poggi, L. *ChemBioChem* **2001**, *2*, 550−558.
(8) Kostic, M.; Pochapsky, S. S.; Pochapsky, T. C. *J. Am. Chem. Soc.* **2002**, *124*, 9054−9055.
(9) Machonkin, T. E.; Westler, W. M.; Markley, J. L. *J. Am. Chem. Soc.* **2002**, *124*, 3204−3205.
(10) Bermel, W.; Bertini, I.; Felli, I. C.; Kummerle, R.; Pierattelli, R. *J. Am. Chem. Soc.* **2003**, *125*, 16423−16429.
(11) Machonkin, T. E.; Westler, W. M.; Markley, J. L. *Inorg. Chem.* **2005**, *44*, 779−797.
(12) Kolczak, U.; Salgado, J.; Siegal, G.; Saraste, M.; Canters, G. W. *Biospectroscopy* **1999**, *5*, 519−532.
(13) Bermel, W.; Bertini, I.; Felli, I. C.; Pierattelli, R.; Vasos, P. R. *J. Magn. Reson.* **2005**, *172*, 324−328.
(14) Bertini, I.; Duma, L.; Felli, I.; Fey, M.; Luchinat, C.; Pierratelli, R.; Vasos, P. *Angew Chem., Int. Ed. Engl.* **2004**, *43*, 2257−2259.

10.1021/ja054902h CCC: $33.50

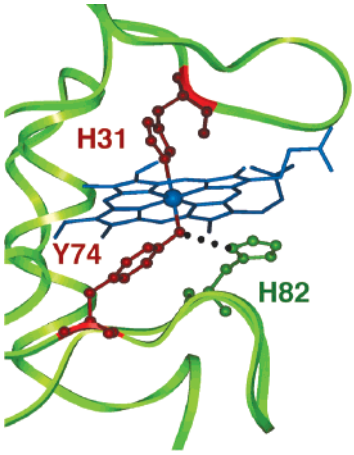

Figure 1. Active-site structure of HasA. The two axial ligands, residues H31 and Y74, are shown in red. The backbone and residue H82 H-bonded to the tyrosine are shown in green.

porter via their carboxy-terminal signal.[15] Their function is to bind free or hemoprotein-bound heme and to deliver it to a specific outer-membrane receptor, HasR.[16] *Serratia marcescens* HasA is a 19 kDa monomeric protein that binds one iron(III) b-type heme with a very high affinity ($K_a = 5.3 \times 10^{10}$ M^{-1}).[17] The X-ray structure of the protein, available for the holo form,[18] shows an original α/β fold in which the α helices are all packed on one side of the molecule, whereas the β strands are packed on the other side. The axial coordination for the heme iron is atypical (Figure 1).

Ligation is provided by the Nϵ2 of a histidine (H31) in the fifth coordination position, and a tyrosine (Y74) is present in the sixth position. Furthermore, the reduction potential of the heme iron (−550 mV) is the lowest reported for the iron(III)/iron(II) pair of a heme protein.[19] This is consistent with the high exposure of heme to the solvent and with the presence of a tyrosinate as the axial ligand, known to decrease the redox potential of the bound metal ion.[20−22] As observed in many heme proteins, two heme orientations rotated by 180° around the $\alpha-\gamma$ meso axis are present.[23−25]

Tyrosine is an unusual ligand in heme proteins. The His/Tyr coordination is exceptional and is only found in very few native proteins, in specific states. It is observed in the alkaline ferric form of some invertebrate hemoglobins,[26−28] in the reduced form of the cytochrome *c* maturation protein CcmE,[29] and in the oxidized form of the cytochrome cd_1 nitrite reductase.[30] A few abnormal human hemoglobins[31] and some mutated heme proteins also present this type of ligation.[32] Besides the H31/Y74 pair of ligands, a third residue was shown to play an important role in heme binding in the hemophore HasA: the histidine H82.[17,33] A H-bond between its Nδ1 and the Y74 Oη was observed in the two crystal structures obtained at pH 4.6 (1B2V) and pH 8.0 (1DKO), respectively.[34] Moreover, as determined by NMR for the gallium(III) derivative of HasA in solution, H82 has a pK_a of 9.7 and shares a proton with Y74 that is stabilized in a coordinating conformation through this H-bond.[33] However, another crystal structure (1DKH) obtained at pH 6.5 reveals a different orientation of H82 in the heme pocket giving rise to a different H-bond network.[34] In this structure, the Nδ1 atom of H82 is involved in a hydrogen bond with a water molecule and no longer with Y74 Oη.

No NMR data are yet available on the paramagnetic iron(III) holoHasA. NMR spectroscopy was previously used to assign backbone and Cβ resonances in the gallium(III)-substituted protein (BMRB number 5081).[35] This derivative, whose NMR data are consistent with the X-ray structures 1B2V and 1DKO, was chosen as a diamagnetic analogue of the holoprotein for this study.

In this paper, we report the NMR characterization of the native paramagnetic iron(III) holoHasA in solution. ^{15}N and ^{13}C direct detection allowed us to approach the very close environment of the iron and to detect resonances of atoms located less than 5 Å from the paramagnetic center. Complete assignment of backbone and Cβ carbon atoms was achieved for 173 residues out of 178. Remarkably, resonances from the two axial ligands and from H82 could be identified.

Materials and Methods

Expression and Purification of the HasA Proteins from *Serratia marcescens*. Wild-type HasA was expressed in *Escherichia coli* strain POP3 transformed with plasmid pSYC34 (pAM238).[36] Y74A and H82A mutants were constructed by in vitro site-directed mutagenesis.[37] Uniformly labeled ^{15}N and $^{15}N/^{13}C$ proteins were produced in M9 minimal medium at 303 K containing $^{15}NH_4Cl$ and ^{13}C−glycerol as the sole nitrogen and carbon sources and were purified as described previously.[19,38] Purity of the proteins was checked by SDS−PAGE.

(15) Letoffe, S.; Ghigo, J. M.; Wandersman, C. *J. Bacteriol.* **1994**, *176*, 5372−5377.
(16) Ghigo, J. M.; Letoffe, S.; Wandersman, C. *J. Bacteriol.* **1997**, *179*, 3572−3579.
(17) Deniau, C.; Gilli, R.; Izadi-Pruneyre, N.; Letoffe, S.; Delepierre, M.; Wandersman, C.; Briand, C.; Lecroisey, A. *Biochemistry* **2003**, *42*, 10627−10633.
(18) Arnoux, P.; Haser, R.; Izadi, N.; Lecroisey, A.; Delepierre, M.; Wandersman, C.; Czjzek, M. *Nat. Struct. Biol.* **1999**, *6*, 516−520.
(19) Izadi, N.; Henry, Y.; Haladjian, J.; Goldberg, M. E.; Wandersman, C.; Delepierre, M.; Lecroisey, A. *Biochemistry* **1997**, *36*, 7050−7057.
(20) Nagai, M.; Yubisui, T.; Yoneyama, Y. *J. Biol. Chem.* **1980**, *255*, 4599−4602.
(21) Dong, A.; Nagai, M.; Yoneyama, Y.; Caughey, W. S. *J. Biol. Chem.* **1994**, *269*, 25365−25368.
(22) Nagai, M.; Mawatari, K.; Nagai, Y.; Horita, S.; Yoneyama, Y.; Hori, H. *Biochem. Biophys. Res. Commun.* **1995**, *210*, 483−490.
(23) Wu, J. Z.; La Mar, G. N.; Yu, L. P.; Lee, K. B.; Walker, F. A.; Chiu, M. L.; Sligar, S. G. *Biochemistry* **1991**, *30*, 2156−2165.
(24) Nguyen, B. D.; Xia, Z.; Cutruzzola, F.; Allocatelli, C. T.; Brunori, M.; La Mar, G. N. *J. Biol. Chem.* **2000**, *275*, 742−751.
(25) Caignan, G. A.; Deshmukh, R.; Wilks, A.; Zeng, Y.; Huang, H. W.; Moenne-Loccoz, P.; Bunce, R. A.; Eastman, M. A.; Rivera, M. *J. Am. Chem. Soc.* **2002**, *124*, 14879−14892.
(26) Kraus, D. W.; Wittenberg, J. B.; Lu, J. F.; Peisach, J. *J. Biol. Chem.* **1990**, *265*, 16054−16059.
(27) Lecomte, J. T.; Smit, J. D.; Winterhalter, K. H.; La Mar, G. N. *J. Mol. Biol.* **1989**, *209*, 235−247.
(28) Das, T. K.; Couture, M.; Lee, H. C.; Peisach, J.; Rousseau, D. L.; Wittenberg, B. A.; Wittenberg, J. B.; Guertin, M. *Biochemistry* **1999**, *38*, 15360−15368.
(29) Uchida, T.; Stevens, J. M.; Daltrop, O.; Harvat, E. M.; Hong, L.; Ferguson, S. J.; Kitagawa, T. *J Biol Chem* **2004**, *279*, 51981−51988.
(30) Williams, P. A.; Fulop, V.; Garman, E. F.; Saunders, N. F.; Ferguson, S. J.; Hajdu, J. *Nature* **1997**, *389*, 406−412.
(31) Nagatomo, S.; Jin, Y.; Nagai, M.; Hori, H.; Kitagawa, T. *Biophys. Chem.* **2002**, *98*, 217−232.
(32) Maurus, R.; Bogumil, R.; Luo, Y.; Tang, H. L.; Smith, M.; Mauk, A. G.; Brayer, G. D. *J. Biol. Chem.* **1994**, *269*, 12606−12610.
(33) Wolff, N.; Deniau, C.; Letoffe, S.; Simenel, C.; Kumar, V.; Stojiljkovic, I.; Wandersman, C.; Delepierre, M.; Lecroisey, A. *Protein Sci.* **2002**, *11*, 757−765.
(34) Arnoux, P.; Haser, R.; Izadi-Pruneyre, N.; Lecroisey, A.; Czjzek, M. *Proteins* **2000**, *41*, 202−210.
(35) Deniau, C.; Couprie, J.; Simenel, C.; Kumar, V.; Stojiljkovic, I.; Wandersman, C.; Delepierre, M.; Lecroisey, A. *J. Biomol. NMR* **2001**, *21*, 189−190.
(36) Létoffé, S.; Ghigo, J. M.; Wandersman, C. *Proc. Natl. Acad. Sci. U.S.A.* **1994**, *91*, 9876−9880.
(37) Letoffe, S.; Deniau, C.; Wolff, N.; Dassa, E.; Delepelaire, P.; Lecroisey, A.; Wandersman, C. *Mol. Microbiol.* **2001**, *41*, 439−450.
(38) Izadi-Pruneyre, N.; Wolff, N.; Castagne, C.; Czisch, M.; Wandersman, C.; Delepierre, M.; Lecroisey, A. *J. Biomol. NMR* **1999**, *14*, 193−194.

The protein concentrations were determined using the previously determined $\epsilon_{277\ nm}$ values of 19 500 M^{-1} cm^{-1} for HasA and 18 500 M^{-1} cm^{-1} for H82A and Y74A mutants. Cleavage of the last nine residues (179−187) of HasA proteins was performed by the *S. marcescens* protease Prt_{SM} to prevent sequential proteolysis of the C terminus, generating new C-terminal amino acids and significant changes in pH.[39]

Preparation of Holoprotein NMR Samples. Bovine hemin (Sigma) was dissolved in a minimal volume of 0.1 N NaOH, centrifuged, and diluted with 20 mM sodium phosphate buffer, pH 7. The concentration of the heme solution was measured in 0.1 N NaOH, using the $\epsilon_{385\ nm}$ value of 58 440 M^{-1} cm^{-1}.[40] Freshly prepared hemin solution was added to the protein with a ratio of about 120%. The excess of heme was eliminated by gel filtration (20 mM phosphate buffer, pH 7) to obtain 100% heme-loaded protein, as monitored by the absence of apoprotein resonances in the $^1H-^{15}N$ HSQC spectra.

NMR Sample Preparation. All samples were in 20 mM phosphate buffer, pH 5.6 and 10% ^2H_2O, except when otherwise mentioned. Concentrations of holoHasAwt were 1 mM for the ^{15}N-labeled sample and 1.6 mM for the ^{13}C- and ^{15}N-labeled one. Concentrations of mutants, ^{15}N-labeled holoH82A and ^{13}C- and ^{15}N-labeled holoY74A, were 1.2 mM and 2 mM, respectively. The pH was adjusted when necessary with 0.1 M HCl or 0.1 M NaOH and systematically controlled after NMR data collection. pH values were not corrected for the deuterium isotope effect.

NMR Spectroscopy. Experiments for direct detection of low γ nuclei were performed on a 16.4 T Bruker AVANCE 700 spectrometer equipped with a triple-resonance probe optimized for ^{13}C direct-detection (TXO) experiments and on a 9.4 T Bruker AVANCE 400 equipped with a double-resonance probe (BBO) for ^{15}N direct-detection experiments.

Two-dimensional ^{13}C-detected CBCACO,[6] CACO,[6] CON,[8] and CANCO[14] were performed to assign diamagnetic backbone C/N and Cβ resonances. All the above experiments were recorded by acquiring $^{13}C'$ during t_2, using spectral windows of 20−25 ppm with the carrier frequency at 175 ppm. Sixteen to 64 scans were collected for each fid using 512 data points for t_2 acquisition, and recycle delays were in the range 1−1.5 s. For the indirect dimension, in CBCACO, 384 points were acquired over 100 ppm with the carrier at 35 ppm. In CACO, 1536 points were acquired over 80 ppm with the carrier at 55 ppm. In CON, 600 data points for the ^{15}N dimension were acquired over 40 ppm with the carrier at 120 ppm. In CANCO, 170 points were acquired over 40 ppm in the Cα dimension with the carrier at 57 ppm. For the last experiment, 1536 scans were used for each fid. All of the above ^{13}C-detected experiments were acquired using the in-phase/anti-phase (IPAP) scheme to avoid C$\alpha-C'$ coupling during carbonyl acquisition.[6] $^{13}C-^{13}C$ correlation spectroscopy (COSY) was performed with 800 × 2048 data points, 64 scans, and a recycle delay of 1 s. Spectral widths of 220 ppm in both dimensions with the carriers at 150 ppm for the indirect dimension and at 110 ppm for the direct dimension were used. Besides $^{13}C-^{13}C$ COSY, which was acquired and processed in magnitude mode, States-time-proportional phase incrementation (TPPI) acquisition[41] was used to perform quadrature detection in the indirect dimension for all the experiments.

Assignment of paramagnetic carbon resonances was made with a single quantum (SQ) antiphase (AP) CACO experiment[42] and with tailored $^{13}C-^{13}C$ COSY.[7] The CACO-SQ-AP experiment was performed with 512 × 256 data points, 512 scans, and a recycle delay of 300 ms. Spectral widths of 80 ppm, with the carrier at 55 ppm for the Cα dimension, and of 25 ppm, with the carrier at 175 ppm for the carbonyl dimension, were used. The delay for the C$\alpha-C'$ insensitive nuclei enhanced by polarization transfer (INEPT) used for detection of diamagnetic resonances was shortened from 4.5 to 2.8 ms.[43] The $^{13}C-^{13}C$ COSY was performed with 2048 × 256 data points, 1024 scans, and a recycle delay of 300 ms. Spectral widths and carriers were the same as the one used for the diamagnetic experiment.

To detect diamagnetic resonances, a $^{15}N-^1H$ heteronuclear single quantum correlation (HSQC) experiment was performed at 400 MHz with 2048 × 512 data points, 16 scans, and a recycle delay of 1 s. Spectral widths of 13 ppm, with the carrier at 4.7 ppm for the ^1H dimension, and of 40 ppm, with the carrier at 120 ppm for the ^{15}N dimension, were used. Quadrature detection in the indirect dimension was performed with echo−antiecho.[44] Two-dimensional $^1H-^{15}N$ HSQC experiments were optimized to detect fast relaxing signals, at 400 MHz. INEPT transfer and recycle delays were shortened to 1 and 300 ms, respectively, to detect resonances near the paramagnetic center. Data points, 220 × 2048, were acquired with 256 scans per increment. Spectral widths and carriers were identical to those previously described for $^1H-^{15}N$ HSQC.

The one-dimensional ^1H NMR spectra were acquired at 700 MHz with a spectral width of 240 ppm and 8192 data points. During the recycle delay of 150 ms, water suppression was achieved by presaturation. The one-dimensional ^{15}N NMR spectra were acquired with a 30 μs 90° pulse, a spectral width of 450 ppm, 2048 data points, and a recycle delay of 10 ms. The one-dimensional ^{13}C NMR spectra were acquired with a 12.4 μs 90° pulse, a spectral width of 500 ppm, and 2048 data points. To identify signals over wide spectral regions, experiments were performed with carriers at 150 and 567 ppm. Recycle delays were 10 and 200 ms. ^{13}C T_1 values have been measured via the inversion recovery sequence. Spectra at variable interpulse delays were acquired, using 100 and 10 ms as recycle delays. Several series were performed with the ^{13}C-carrier frequency at different positions, to properly invert and excite all ^{13}C resonances. Unless otherwise specified, NMR spectra were recorded at 303 K.

Magnetic Susceptibility Tensor Calculations. Pseudocontact shifts arise from the magnetic susceptibility anisotropy and depend on the nuclear position with respect to the principal axes of the magnetic susceptibility tensor, according to the following equation:[45]

$$\delta_i^{pc} = \frac{1}{12\pi r_i^3}\left[\Delta\chi^{para}_{ax}(3n_i^2 - 1) + \frac{3}{2}\Delta\chi^{para}_{rh}(l_i^2 - m_i^2)\right] \quad (1)$$

where $\Delta\chi^{para}_{ax}$ and $\Delta\chi^{para}_{rh}$ are the axial and rhombic anisotropies of the magnetic susceptibility tensor, l_i, m_i, and n_i are the cosine directions of the position vector of atom i with respect to the magnetic susceptibility tensor coordinate system, and r_i is the distance between the paramagnetic center and the nucleus i. Therefore, the measurement of the pseudocontact shift for tens of nuclei provides an accurate estimate of the magnetic anisotropy and of the directions of the magnetic susceptibility tensor axes within the protein frame. Two different magnetic anisotropy tensors were built with the coordinates of 1B2V (Y74−H82 hydrogen bond) and 1DKH (no Y74−H82 hydrogen bond) structures.[34]

In addition to a pseudocontact shift, nuclei connected through few chemical bonds to the metal ion may experience a contact shift.[46] Pseudocontact shifts from all residues but H31, H82, and Y74 were determined by subtracting from the observed shifts in the iron(III) derivative the observed shifts of the analogous diamagnetic gallium(III) derivative, and then they were used for tensor calculations.

The list of N, HN, C′, Cα, and Cβ nuclei used for tensor calculations is reported in the Supporting Information (Table S1).

(39) Izadi-Pruneyre, N.; Wolff, N.; Redeker, V.; Wandersman, C.; Delepierre, M.; Lecroisey, A. *Eur. J. Biochem.* **1999**, *261*, 562−568.
(40) Dawson, R. M. C.; Elliott, D. C.; Elliott, W. H.; Jones, K. M. Oxford University Press: New York, 1986; pp 233−236.
(41) Marion, D.; Wuthrich, K. *Biochem. Biophys. Res. Commun.* **1983**, *113*, 967−974.
(42) Bertini, I.; Jimenez, B.; Piccioli, M. *J. Magn. Reson.* **2005**, *174*, 125−132.
(43) Piccioli, M.; Poggi, L. *J. Magn. Reson.* **2002**, *155*, 236−243.
(44) Kay, L. E.; Keifer, P.; Saarinen, T. *J. Am. Chem. Soc.* **1992**, *114*, 10663−10665.
(45) Kurland, R. J.; Macgarvey, B. R. *J. Magn. Reson.* **1970**, *2*, 286−301.
(46) McConnell, H. M.; Chesnut, D. B. *J. Chem. Phys.* **1958**, *28*, 107−117.

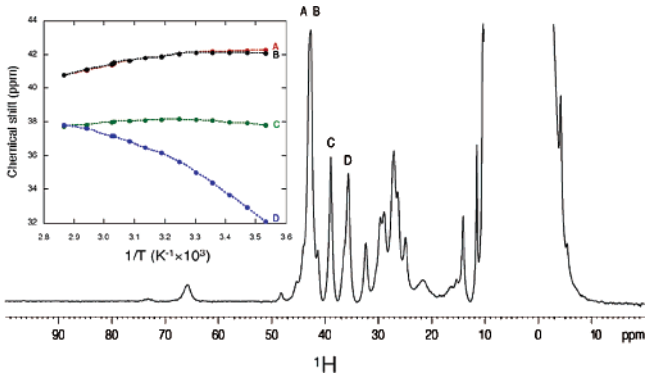

Figure 2. ^{1}H NMR spectrum of holoHasA recorded at 700 MHz and 303 K in 20 mM phosphate buffer, pH 5.6. The inset shows the temperature dependence of the chemical shift for heme methyl resonances.

Results and Discussion

Chemical Equilibrium between Different Iron Spin States. The one-dimensional ^{1}H NMR spectrum of holoHasA (Figure 2) shows the presence of two sets of resonances in a 70:30 ratio, corresponding to the two possible orientations of the heme along the $\alpha-\gamma$ meso axis, as observed in the crystal structure.

The four more intense signals permit us to identify the four methyl heme resonances of the major form. They are observed at 42.7 (two overlapping signals at 303 K), 38.9, and 35.7 ppm. The average chemical shift for heme methyls (ca. 40 ppm) is intermediate between typical values of a purely high-spin, $S = 5/2$, heme iron(III) and those of a purely low-spin, $S = 1/2$, heme iron(III). T_1 values are 8−9 ms, and line widths are about 400 Hz. Similar average chemical shifts for heme methyl resonances have already been observed in different hemoproteins such as the V68H and H64V/V68H myoglobin mutants,[47,48] the *E. coli* ferricytochrome b_{562},[23] or the *c* domain of *Paracoccus pantotrophus* cytochrome cd1 nitrite reductase[49] together with short T_1 values in most of these systems. In all cases, a high-spin/low-spin equilibrium has been established. We therefore propose that a chemical equilibrium between a high-spin and a low-spin species also occurs in HasA. An exchange, fast on the chemical shift NMR time scale, explains the average chemical shift observed. The analysis of the temperature dependence of the chemical shifts of heme methyl resonances (signals A, B, C, and D in Figure 2) shows a nonlinear behavior (inset to Figure 2). This deviation from Curie behavior indicates that the relative populations of the two species change with temperature and gives additional evidence for a spin-state equilibrium. At higher temperature, the high-spin state becomes more populated and shifts of the heme methyls tend toward the values expected for pure high-spin species. Simultaneously, as the shifts for pure high-spin species follow the Curie law, they tend toward their diamagnetic values with increasing temperature. The balance between the two effects is different for each methyl. Because signal D at 303 K has a lower hyperfine shift than the others, it shows the largest increase in chemical shift in the observed range (Figure 2, inset). The temperature dependence of ^{13}C ligand resonances also supports this view (see later).

(47) Lloyd, E.; Hildebrand, D. P.; Tu, K. M.; Mauk, A. G. *J. Am. Chem. Soc.* **1995**, *117*, 6434−6438.
(48) Qin, J.; La Mar, G. N.; Dou, Y.; Admiraal, S. J.; Ikeda-Saito, M. *J. Biol. Chem.* **1994**, *269*, 1083−1090.
(49) Steensma, E.; Gordon, E.; Oster, L. M.; Ferguson, S. J.; Hajdu, J. *J. Biol. Chem.* **2001**, *276*, 5846−5855.

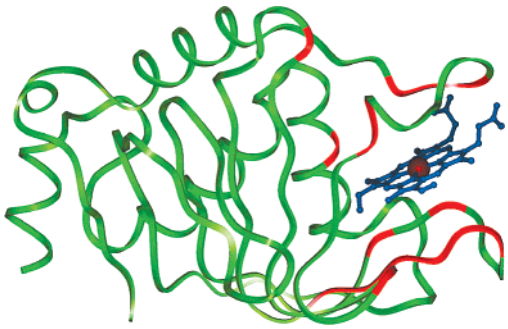

Figure 3. Display of the structure of HasA (PDB id 1B2V). The residues not or weakly affected by the iron are shown in green. The residues which present fast relaxing signals are shown in red. The b-heme is in blue, and the heme iron is in red.

Assignment Strategy. The cleaved form of holoHasA comprises residues 1−178. We aimed at a complete assignment of holoHasA resonances and, in particular, at identifying signals of nuclei that are strongly affected by the proximity of the metal ion. Short T_1 values for protons close to the paramagnetic center prevented us from using classical ^{1}H NMR experiments for the assignment of resonances in the immediate proximity of the heme iron(III). We therefore used mainly ^{13}C direct-detection experiments for the assignment of both the paramagnetic and the diamagnetic resonances of the protein.

Depending on the distance from the metal center, different approaches were used to perform sequence-specific assignments, as described in the following sections.

A. Assignment of Diamagnetic Signals. The assignment of nuclei from residues located relatively far from the iron ion (residues in green in Figure 3) was achieved using a ^{15}N-enriched sample through a ^{15}N−^{1}H HSQC experiment and a ^{13}C−^{15}N-enriched sample through two-dimensional ^{13}C-detected double-resonance experiments.

Advantage was taken of the previously reported assignment of the diamagnetic gallium protoporphyrin IX derivative.[35] The assignment of the paramagnetic iron(III) holoHasA was performed through a minimal set of experiments constituted by ^{15}N−^{1}H HSQC and by the recently developed CACO, CBCACO, CON, and CANCO.[6] Most of the N/HN backbone resonances could be assigned by simply comparing the ^{15}N−^{1}H HSQC spectra of both gallium(III) and iron(III) holoHasA. CACO and CBCACO spectra were assigned referring to chemical shifts of the Cα, Cβ, and C′ nuclei of gallium(III) holoHasA. Sequential connectivities were confirmed via two-dimensional CANCO and CON experiments that also helped in resolving ambiguities due to overlapping peaks.

The ^{1}H−^{15}N HSQC (Figure 4A) experiment allowed the identification of 159 backbone N and NH resonances. In this spectrum, we could also observe resonances of nuclei at distances lower than 11 Å from the iron: the ^{15}N and ^{1}H amides from residues 30, 34, 35, 38, 42, 43, 78, 81, 85, 136, and 139 at distances between 9.5 and 11.0 Å and those from residues 36 and 37 at 8.1 and 8.6 Å, respectively. Missing residues were the N-terminal, the 3 prolines, and 15 residues close to the paramagnetic center: residues 31−33, 40, 41, 49, 59, 73−77, and 82−84.

The CACO and CBCACO experiments allowed us to fully assign the C′, Cα, and Cβ resonances of 167 residues and to partially assign those of six residues, namely, N40, S41, S48,

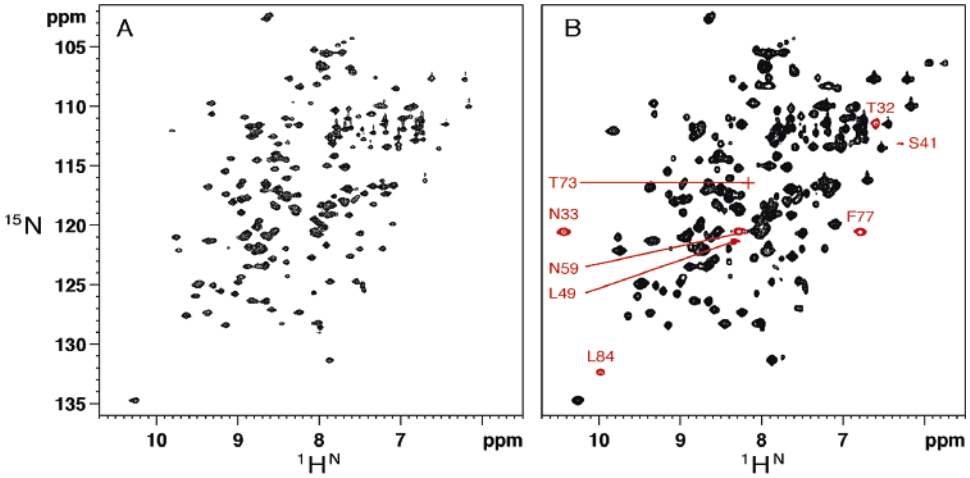

Figure 4. ^{1}H−^{15}N HSQC spectra recorded at 400 MHz with 1 mM aqueous solution of ^{15}N holoHasAwt at 303 K and pH 5.6. Shown is the comparison of the diamagnetic ^{1}H−^{15}N HSQC with a recycle delay of 1 s (A) and the paramagnetic ^{1}H−^{15}N HSQC with a recycle delay of 300 ms to detect fast relaxing signals (B). Extra signals are present in B. A cross represents the ^{1}H−^{15}N correlation of T73 which is not visualized at this threshold.

L72, F77, and Y136. No carbon resonances were detected for residues H31, Y74, L76, H82, and G70. The assignment of most of these residues was confirmed by CON and CANCO experiments, which also permitted us to detect the carbonyl of G70. Indeed, these experiments, which need longer transfer delays, are more sensitive than the CACO and CBCACO experiments to paramagnetism that induces quenching of coherence transfer. Thus, even relatively small relaxation rate enhancements due to paramagnetic contributions are sufficient to quench the transfer between the amide N and the previous carbonyl.[50]

For all the nuclei assigned above, the observed chemical shift differences between the iron(III) and gallium(III) forms of holoHasA are on average ≤0.25 ppm for ^{1}H, ≤0.30 ppm for ^{15}N, and ≤0.60 ppm for ^{13}C. The obtained assignments are reported in the Supporting Information, Table S1.

B. Approaching the Heme Center. To observe the backbone resonances of residues closer to the paramagnetic center (residues in red in Figure 3), faster repetition rates and INEPT delays shorter than those used for standard experiments were required. The paramagnetic tailored ^{1}H−^{15}N HSQC (Figure 4B) allowed detection of eight new peaks corresponding to residues T32, N33, S41, L49, T59, T73, F77, and L84. Only seven, non N-term, non proline, residues remained unidentified: H31, N40, Y74, T75, L76, H82, and T83.

As ^{1}H experiments, ^{13}C-detected double-resonance experiments can be optimized to observe fast relaxing resonances. In the paramagnetic CACO spectra,[42] we could detect cross-peaks, unobservable in diamagnetic spectra, for residues N40 (weak), S41, and H82. The paramagnetic tailored ^{13}C−^{13}C COSY experiment allowed us to identify a few more resonances: Cβ of N40, Cα of S48, Cβ of L72, Cβ and Cγ of H82, and Cβ of Y136. The Cβ and Cγ resonances of H82, which are only about 4.5 Å away from the Fe(III), could be unambiguously assigned in the clean and interesting region of the ^{13}C−^{13}C COSY spectrum which contains the Cβ−Cγ correlations of aromatic residues (Figure 5A). To confirm the assignment of the H82 nuclei, we also checked that the corresponding resonances were not present on diamagnetic ^{13}C−^{13}C COSY (Figure 5B).

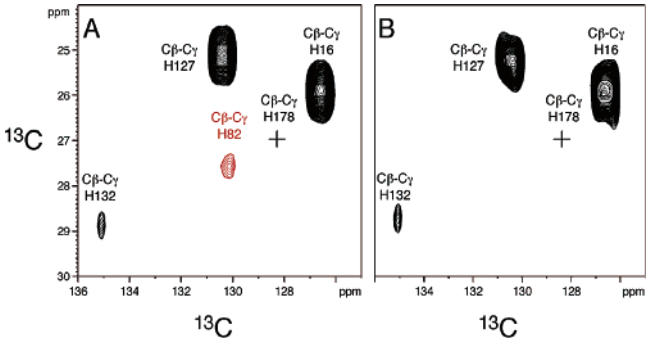

Figure 5. Part of two-dimensional ^{13}C−^{13}C spectra containing Cβ−Cγ correlations of aromatic histidine residues acquired at 700 MHz on holoHasA. The paramagnetic tailored ^{13}C−^{13}C COSY (A) and the diamagnetic ^{13}C−^{13}C COSY (B) are shown. An extended cleavage of the C-terminal of HasA prevents the detection of Cβ−Cγ H178 correlation (Izadi-Pruneyre et al., 1999).

Signals from residues close to the paramagnetic center experience differences in chemical shift and/or line broadening with respect to the corresponding resonances in gallium(III) HasA. Nevertheless, most of them are detectable in paramagnetic experiments. With the ^{13}C−^{13}C COSY and the CACO spectra, we were able to identify the ^{13}C resonances of three residues for which no ^{15}N resonances could be detected in paramagnetic ^{1}H−^{15}N HSQC spectra: N40, T75, and H82. Only three residues remained unidentified: the two axial ligands, Y74 and H31, and a residue close to the tyrosine, L76. In addition to the resonances of these residues, the only unassigned ^{13}C resonances were the Cα of G70 and the Cβ of F77.

Among the assigned residues, T32, N33, S41, L72, T73, H82, and Y136 are the most affected by the presence of the paramagnetic center. At least one of their nuclei resonances shows a large change in chemical shift with respect to the diamagnetic gallium(III) derivative. Hyperfine shifts for the assigned nuclei of these residues range from −1.24 to + 1.10 ppm for ^{15}N, from −0.33 to +7.05 ppm for ^{13}C, and from +0.07 to +0.57 ppm for amide protons, as shown in Supporting Information Table S1. These chemical shift variations are ascribed to nonnegligible pseudocontact shifts, except for H82 which might experience both pseudocontact and contact shifts

(50) Gelis, I.; Katsaros, N.; Luchinat, C.; Piccioli, M.; Poggi, L. *Eur. J. Biochem.* **2003**, *270*, 600−609.

due to its probable H-bond with the axial ligand Y74 in iron(III) holoHasA solutions.

C. Magnetic Anisotropy Tensor. From the hyperfine shift of the nuclei of residues that do not bind the metal, it is in principle possible to evaluate the magnetic anisotropy tensor due to the presence of the paramagnetic metal ion, using the approach already described in the literature.[51] This methodology has also been extensively used to include pseudocontact shifts as nonconventional constraints for solution-structure calculations or to obtain information about the conformation of a protein in solution starting from an X-ray structure in low-spin iron(III) and high-spin iron(II) and iron(III) heme proteins.[52−56] In the present case, the solution-structure determination of the whole protein is out of the scope of the research, as several structures for the whole protein are already available. However, a controversial point of the HasA structure lies in the orientation of H82 and in the presence of a H-bond between its imidazole ring and Y74. With the aim to unravel the average conformation of H82 in solution in the case of the iron(III) protein, we have evaluated the average magnetic susceptibility tensor parameters of iron(III) HasA and used them to gain information on the status of H82, comparing our experimental findings with the two limit structures, 1B2V and 1DKH.

We used a set of 161 backbone NH, 161 amide N, 164 Cα, 166 C′, and 137 Cβ nuclei together with the high-resolution (1.9 Å) X-ray structure 1B2V of the iron protein, determined at pH 4.6 from residues 1−173, as a reference structure (eq 1). The resulting magnetic anisotropy tensor parameters are reported in Supporting Information Table S1. The tensor is well defined, with $\Delta\chi_{ax} = 0.679 \times 10^{-32}$ m^3 and $\Delta\chi_{rh} = -0.431 \times 10^{-32}$ m^3. Tensor parameters were also calculated using the 1DKH structure as a reference. The result is only slightly different, with $\Delta\chi_{ax} = 0.598 \times 10^{-32}$ m^3 and $\Delta\chi_{rh} = -0.371 \times 10^{-32}$ m^3. The major difference between the 1DKH structure and the 1B2V structure lies in the absence of an H82−Y74 H-bond. The hyperfine shifts of the resonances of these two residues, H82 and Y74, as well as those of H31 are not included in tensor calculations because these residues could have nonnegligible contact contributions. In high-spin iron(III) proteins, $\Delta\chi_{ax}$ is typically in the -2.9×10^{-32} to -4.3×10^{-32} m^3 range and $\Delta\chi_{rh}$ is of the order 1.5×10^{-32} m^3.[57,58] Typical magnetic susceptibility anisotropy values in low-spin heme proteins are in the 2.7×10^{-32} to 3.6×10^{-32} m^3 range for $\Delta\chi_{ax}$ and in the 0.9×10^{-32} to 3.6×10^{-32} m^3 range for $\Delta\chi_{rh}$.[54,59,60]

The values determined here for HasA are consistent with the presence of a chemical equilibrium between a low-spin and a high-spin species, in which the resulting tensor represents the vectorial average of the two single tensors. This is why, for example, the average axial magnetic susceptibility anisotropy in HasA is so small; it results from the difference of two large values in opposite directions, characteristic of the two different spin states. It is impossible to attribute a precise physical meaning to the values of the magnetic anisotropies and magnetic axes orientation because only an average value of the magnetic susceptibility tensor parameters is experimentally available. However, the obtained tensor can be used to back-calculate the expected pseudocontact shift contribution to the hyperfine shift for the H31, Y74, and H82 nuclei.

D. Key Residues of the Heme Binding Site: H31, Y74, and H82. Although ^{13}C experiments have been proven to be much more robust for paramagnetism than the standard assignment strategy based on ^1H-detected experiments, the residues bound to the heme escape detection and only the assignment of H82 was available. An alternative strategy which has been extensively used in paramagnetic proteins is the identification of ^1H signals in the proximity of the heme via $^1H-^1H$ nuclear Overhauser enhancement spectroscopy (NOESY) experiments.[61,62] However, in the present case, the short T_1 values of ^1H hyperfine-shifted signals prevent the exploitation of $^1H-^1H$ NOESY experiments. Therefore, we rely on the identification of ^{13}C and ^{15}N signals observed in one-dimensional experiments. Significant hyperfine contact shifts should be observed for residues bound to the heme iron, thus giving hints for their assignment.

D.1. ^{15}N One-Dimensional Spectra. We used one-dimensional ^{15}N direct detection for the identification of the imidazole nitrogen atoms of His residues, with the aim to assign the ^{15}N nuclei of the axial ligand H31 and of the key residue H82. Major and minor sets of signals are observed in the one-dimensional ^{15}N spectrum of holoHasA because of the two possible orientations of the heme in the protein (Figure 6A). Five histidine residues are expected in the cleaved protein. Although H16, H127, and H132 could be easily identified by comparison with the already available assignment of the gallium(III) derivative of HasA,[33] the assignment of H82 and H31 resonances was less straightforward. The H82 Nϵ2 in the major and minor forms was assigned to two relatively sharp (around 20 Hz) signals at about 179 ppm (178.8 and 180.2 ppm, respectively, at pH 7 and 303 K). The corresponding spectrum recorded on the H82A mutant was used to support this conclusion. Indeed, as shown Figure 6C, both signals disappear in the one-dimensional ^{15}N spectrum of the mutant recorded under analogous conditions. The shift value for the H82 Nϵ2 resonance of the major form in the iron(III) wild-type protein differs by +12.9 ppm with respect to that of the gallium(III) protein.[33] A similar effect is observed for the Cβ of H82, which experiences a +7.05 ppm chemical shift difference with respect to the gallium(III) form (Figure 5A). The little sensitivity of the ^{13}C chemical shift to the local environment of the nucleus rules out the idea that the above chemical shift changes could be due to structural variations with respect to the gallium protein. Furthermore, the observed chemical shift differences cannot be accounted for simply on the basis of pseudocontact shift contributions. Indeed, H82 Nϵ2 pseudocontact shifts calculated with the two tensors obtained with 1B2V (Y74−H82 H-bonded

(51) Emerson, S. D.; La Mar, G. N. *Biochemistry* **1990**, *29*, 1556−1566.
(52) Baistrocchi, P.; Banci, L.; Bertini, I.; Turano, P.; Bren, K. L.; Gray, H. B. *Biochemistry* **1996**, *35*, 13788−13796.
(53) Banci, L.; Bertini, I.; Bren, K. L.; Cremonini, M. A.; Gray, H. B.; Luchinat, C.; Turano, P. *J. Biol. Inorg. Chem.* **1996**, *1*, 117−126.
(54) Banci, L.; Bertini, I.; Bren, K. L.; Gray, H. B.; Sompornpisut, P.; Turano, P. *Biochemistry* **1997**, *36*, 8992−9001.
(55) Gochin, M.; Roder, H. *Protein Sci.* **1995**, *4*, 296−305.
(56) Tu, K.; Gochin, M. *J. Am. Chem. Soc.* **1999**, *121*, 9276−9285.
(57) Turano, P.; Battaini, G.; Casella, L. *Chem. Phys. Lett.* **2003**, *373*, 460−463.
(58) De Ropp, J. S.; Thanabal, V.; La Mar, G. N. *J. Am. Chem. Soc.* **1985**, *107*, 8268−8270.
(59) Banci, L.; Bertini, I.; Rosato, A.; Scacchieri, S. *Eur. J. Biochem.* **2000**, *267*, 755−766.
(60) Banci, L.; Bertini, I.; Pierattelli, R.; Tien, M.; Vila, A. J. *J. Am. Chem. Soc.* **1995**, *117*, 8659−8667.
(61) Bertini, I.; Capozzi, F.; Ciurli, S.; Luchinat, C.; Messori, L.; Piccioli, M. *J. Am. Chem. Soc.* **1992**, *114*, 3332−3340.
(62) Sette, M. D. R., J. S.; Hernandez, G.; La Mar, G. N. *J. Am. Chem. Soc.* **1993**, *115*, 5237−5245.

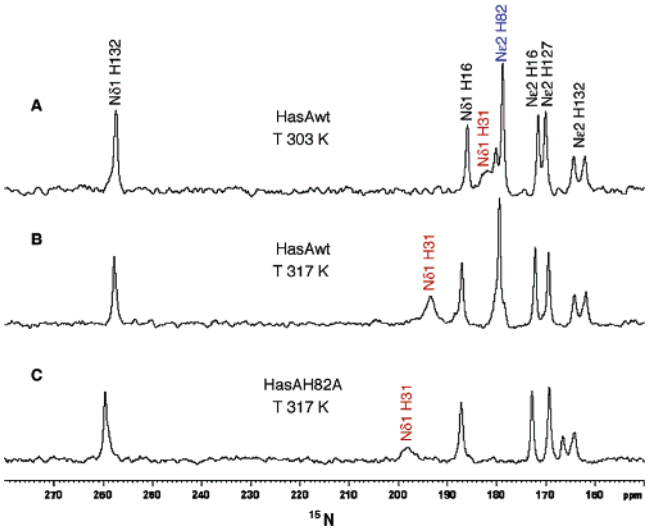

Figure 6. ^{1}H-undecoupled ^{15}N NMR spectra of uniformly ^{15}N-labeled proteins. HasAwt (1 mM) at 303 K (2.47 millions of scans) (A), at 317 K (2.60 millions of scans) (B), 1.2 mM HasA H82A at 317 K (4.89 millions of scans) (C), pH 7. Nϵ2 H132 signal is a doublet. Nδ1 H127 signal appears when pH decreases (173.7 and 182.9 ppm in HasAwt and HasA H82A spectra, respectively, at pH 5.5, 317 K). Nϵ2 H82 signals (blue) disappear in HasA H82A spectrum (C), and Nδ1 H31 signal (red) is present in all spectra with a high temperature dependence.

conformation) and 1DKH (non-H-bonded conformation) structures as references, are, respectively, +0.43 and +0.52 ppm, whereas the δ_{pc} values obtained for the H82 Cβ with the 1B2V and 1DKH tensors are +0.22 and −0.84 ppm, respectively. The large chemical shift differences in the ^{15}N and ^{13}C of H82 between gallium(III) and iron(III) forms can therefore be explained by contact effects contributing to the observed shifts, operative thanks to the presence of a H-bond between H82 Nδ1 and the iron-ligated Y74 Oη, allowing the delocalization of the iron(III) unpaired spin density onto the imidazole ring of H82. The usual Curie behavior would predict, in the 303−317 K temperature range, a −1 to −2 ppm chemical shift change for contact shifts of 10−20 ppm. The +0.7 ppm change observed for H82 Nϵ2 can be explained by a compensatory effect due to a temperature-dependent change of the ^{15}N diamagnetic chemical shift, as observed for the signals of the His residues far from the iron center (Figure 6A,B). Unpaired spin-density transfer from the ligand to the second coordination sphere nuclei has already been reported. It was observed, for example, in the cases of the cyanide low-spin iron(III) adducts of M80A cytochrome *c*[63] and the *Paramphistomum epiclitum* hemoglobin[64] for the hydroxyl proton of a tyrosine H-bonded to the cyanide ligand. In the case of both iron(III) and iron(II) forms of the iron sulfur protein *Clostridium pasteurianum* rubredoxin, ^{15}N shifts of up to 600 ppm were observed for residues not directly bound to the metal. They were related to unpaired spin density provided by the extended H-bonding network between the Sγ donor of the four coordinated cysteines and the HN of hydrophobic residues of the iron binding loop.[65]

A broad signal, about 70 Hz, is observed under the H82 Nϵ2 resonance at 181.2 ppm in the one-dimensional ^{15}N spectrum

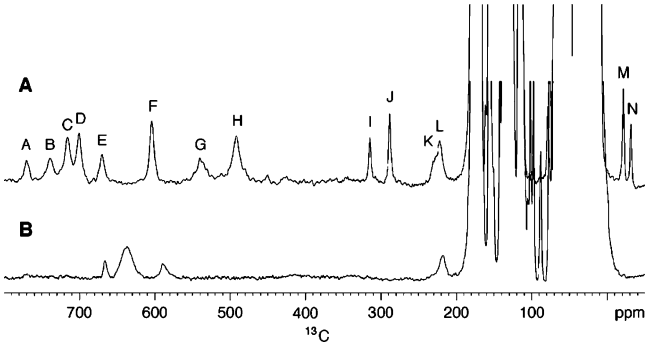

Figure 7. ^{13}C NMR spectra of HasAwt (A) and HasA Y74A (B) obtained at 303 K, pH 5.6.

of holoHasA (Figure 6A). The chemical shift of this broad resonance changes from 181.2 ppm at 303 K to 193.4 ppm at 317 K (Figure 6B). The strong temperature dependence and the absence of an analogous signal in the gallium(III) form suggest that this signal arises from a nucleus very close to the iron, i.e., belonging to H31 or H82. This resonance is also present in the one-dimensional ^{15}N spectra of the holoH82A mutant (Figure 6C). Thus, it was assigned to the Nδ1 of H31. Two close signals were also expected for Nδ1 of H31 because of the two heme orientations. However, because of the probable small chemical shift difference together with the large line widths, they might be overlapped and only one broad resonance could be detected. The observed chemical shift for H31 Nδ1 at 303 K corresponds to about +17 ppm of hyperfine shift, and the expected pseudocontact contribution is about −3 ppm only. Therefore, a +20 ppm contact shift should be operative. The strong anti-Curie temperature dependence of this ^{15}N resonance is similar to that already described for ^{1}H chemical shifts of heme CH_3 groups and is consistent with the fact that H31 experiences a larger contact shift in the high-spin form, favored at higher temperatures. The H31 Nδ1 signal is much broader than the other ^{15}N resonances, as expected for a heme iron ligand. Consistently, the resonances of H31 Nϵ2 are expected to be broadened beyond detection because of its shorter distance to iron and to its direct bonding with the paramagnetic center.

Finally, the H82 Nδ1 resonance could not be observed. This may be due to a relatively large hyperfine shift contribution that may shift it beneath other resonances in the ^{15}N spectrum and/or to increased line width due to contact effects. Both phenomena are consistent with the delocalization of the unpaired spin through the H-bond H82 Nδ1−Y74 Oη.

D.2. One-Dimensional ^{13}C Spectra. Direct detection of ^{13}C nuclei in one-dimensional NMR experiments allowed us to observe resonances that are shifted very far from the typical diamagnetic region. We successfully used this route to determine the ^{13}C resonances of the two axial ligands, Y74 and H31. The one-dimensional ^{13}C spectrum of holoHasA shows fourteen well-resolved peaks (labeled A−N in Figure 7A) that appear to be hyperfine shifted. Twelve resonances (signals A−L) are observed downfield in the 220−770 ppm region (Figure 7A), and two other signals (M and N) are observed upfield, at about −22 and −32 ppm. The T_1 values of all these signals could be determined by non selective inversion recovery experiments. The T_1 values of the downfield signals are in the range of 1−13 ms, and larger T_1 values of 86 and 71 ms are found for the upfield signals M and N, respectively (Table 1).

(63) Bren, K. L.; Gray, H. B.; Banci, L.; Bertini, I.; Turano, P. *J. Am. Chem. Soc.* **1995**, *117*, 8067−8073.
(64) Du, W.; Xia, Z.; Dewilde, S.; Moens, L.; La Mar, G. N. *Eur. J. Biochem.* **2003**, *270*, 2707−2720.
(65) XIA, B.; Westler, W. M.; Cheng, H.; Meyer, J.; Moulis, J. M.; Markley, J. L. *J. Am. Chem. Soc.* **1995**, *117*, 5347−5350.

Table 1. Properties of Hyperfine-Shifted ^{13}C NMR Signals of Iron(III) HasA Wild-Type from *Serratia marcescens*

peak	δ (ppm) 303 K	T_1 (ms)	$\Delta\nu$ (Hz)	shift on increasing temperature
A	769.4	1	1200	upfield
B	738.0	3	1100	upfield
C	714.5	1	750	upfield
D	700.1	2	750	upfield
E	669.2	1	850	downfield
F	603.4	3	850	downfield
G	538.0	1	1600	downfield
H	491.9	1	1400	downfield
I	314.2	8	400	downfield
J	288.1	13	400	downfield
K	228.2	6	1200	downfield
L	222.1	nd[a]	1200	downfield
M	−21.9	86	350	upfield
N	−31.8	71	350	upfield

[a] nd: not determined.

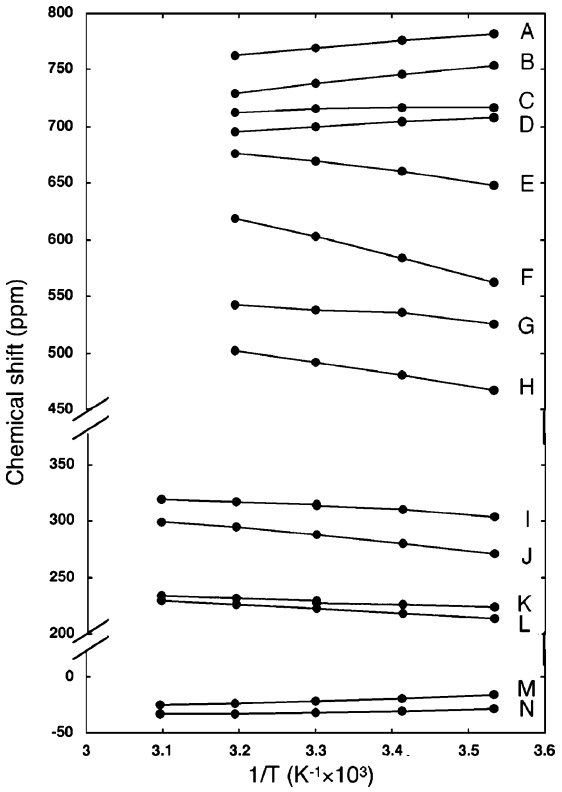

Figure 8. Curie plot of the hyperfine-shifted ^{13}C NMR signals.

Signals A−N show a marked temperature dependence (Figure 8). The chemical shift, T_1, and line width values of the observed signals can only be consistent with the hypothesis that they belong to the coordination environment of the iron. As the heme is not ^{13}C labeled, they should belong to the axial ligands Y74 and H31 or to H82 (Table 1). The large number of detected signals arises from the two different heme orientations previously described, and the intensity ratio between the two sets is similar to that of the ^1H NMR spectrum performed on the same sample. A set of major signals can be identified on the basis of the relative intensity of signals A−N: C, D, F, H, J, L, and M. In an effort to specifically identify these resonances, we recorded the one-dimensional spectrum of the Y74A mutant, which is reported in Figure 7B. From the comparison of the ^{13}C spectra of both WT and Y74A mutants, we observe that six fast relaxing and well-shifted signals are retained in the Y74A derivative. Consistently, they belong to the H31 axial ligand.

The temperature dependence of the chemical shift of the hyperfine-shifted ^{13}C signals of HasA, which is shown in Figure 8, is peculiar. None of the signals display a linear temperature dependency. As already discussed for the ^1H chemical shifts of the heme methyls, the behavior of those resonances whose hyperfine shift increases at increasing temperatures can be rationalized assuming a temperature-dependent chemical equilibrium between two spin states: a low-spin species, $S = 1/2$, and a high-spin species, $S = 5/2$, characterized by substantially larger hyperfine shifts, with the latter species becoming more populated at higher temperature.

The presence of a high-spin species for the heme iron(III) in HasA can be consistent with a release of the axial Y74 ligand upon increasing temperature, thus leaving a pentacoordinated species or a six-coordinated species with a water molecule as the sixth ligand. The absence of the coordinated Y74 is also found to give rise to a high-spin form (unpublished results). The high-spin species in HasA could also be consistent with a significant weakening of the Y74−iron bond modulated by the strength of the Y74−H82 hydrogen bond. Upon breaking or weakening of the coordination bond between the iron and the Tyr, the nuclei of the latter residue would experience no more or very little contact shift. In this frame, the apparent Curie behavior for resonances labeled A, B, C, and D would be interpreted, assuming that they belong to Y74 and that, therefore, their shift tends toward their diamagnetic values upon increasing the population of the high-spin species.

The fact that the Tyr resonances do experience a larger hyperfine shift than the His resonances is not inconsistent with the fact that the Y74−iron bond is weaker than the H31−iron bond because the delocalization mechanism on the two rings is different. In particular, it has been demonstrated in the cases of pyridine and pyridine-*N*-oxide that coordination through the oxygen increases the hyperfine shift on the pyridine ring through π mechanisms.[66] The assignment of the other two pairs of resonances (I and J and M and N) to either of the two axial ligands remains more doubtful.

Conclusions

The ^{13}C NMR characterization of iron(III) HasA represents a seminal example of the use of advanced NMR methodologies for obtaining structural information of biological relevance.

The introduction of low γ nuclei direct detection has been shown to be essential to identify heme binding residues in a highly paramagnetic iron(III) heme protein. Complete assignment of backbone and Cβ resonances for 163 out of 178 residues and partial assignment for twelve of the remaining residues were obtained. The only unassigned residues were the two iron ligands, H31 and Y74, as well as L76. Still, some of their resonances could be observed in one-dimensional ^{15}N and ^{13}C experiments.

Although the per-atom assignment of the two axial ligands was not possible, this is the first time that the ^{13}C resonances of the iron-coordinated residues of a heavily paramagnetic heme iron(III) are detected. The very fast relaxation rates of the signals of the two ligands prevented us from any nucleus-specific

(66) Drago, R. S. P., W. D.; Herlocker, W.; Pagenkopf, G. K.; Czworniak, K. *Inorg. Chem.* **1971**, *10*, 1087−1090.

assignment; both $^{13}C-^{13}C$ nuclear Overhauser effect (NOE)[67] and $^{13}C-^{13}C$ COSY[7] experiments tailored to identify connectivities involving the most shifted signals of the ^{13}C spectrum were unsuccessful. Nevertheless, some important insights on the origin of such resonances were obtained from the analysis of the temperature dependence of their shift values. Indeed, besides being useful for the per-residue assignment of most of the hyperfine-shifted resonances of the ^{13}C spectrum, this dependence was used to infer the structural origin of the high-spin/low-spin equilibrium in solution, which consists of the breaking or the weakening of the Y74 Oη−heme iron bond. The fact that the equilibrium between the two species is fast on the chemical shift time scale suggests that the energy barrier for the transition is low, as would be reasonable if the removal or the weakening of the coordination bond does not involve important conformational changes.

In this protein, multiple factors may contribute to the weakness of the sixth coordination bond: (i) Tyr is per se not a good metal ligand in proteins and has to be stabilized in a coordinating conformation. Here, H82 provides this stabilization through a H-bond between its Nδ1 and the tyrosinate Oη. (ii) The same H-bond not only has a steric effect but also increases the tyrosinate character of Y74, thus making it a stronger ligand. (iii) Both Y74 and H82 belong to a long loop that is expected to be largely flexible in solution, which can induce modulations in the H82 Nδ1 and Y74 Oη hydrogen bond strength and in the tyrosine protonation state.

HasA is a heme carrier and, as such, has to bind and release the heme under the appropriated circumstances. The comparison of the average heme methyl chemical shift value in HasA with those typical for low-spin heme iron(III) (15−20 ppm) and high-spin heme iron(III) proteins (60−70 ppm) suggests that the protein in solution at room temperature functions with only about 50% of strong tyrosine ligation. This ratio remains a rough estimate of the relative population of the two states because we do not have access to the chemical shift values of the two limit spin states in the present systems, but in any case, the high-spin population is significant. Although the low-spin state has a histidine and a tyrosinate as ligands, the high-spin state has a weak, if no, sixth ligand. The affinity of the high-spin species for heme is most likely lower than that of the low-spin species and lower than that determined previously for HasA (about 5 pM), which is the average between the affinities of the two species. HasA has a higher affinity for heme than its receptor HasR (about 1 μM),[68] which raises the question of the heme transfer from a high-affinity protein to a lower-affinity protein. We propose that, upon binding HasR, the high-spin/low-spin equilibrium shifts toward the high-spin species. The affinity of HasA for heme in the complex HasA−HasR would become lower than that of HasR, thus allowing heme transfer.

Acknowledgment. We thank C. Wandersman for constant interest in this work. This research was financially supported by "Ministère de l'éducation nationale et de la recherche" and by "Ministero Italiano dell' Universita' e della Ricerca" PRIN-2003. During her permanence at CERM, C. Caillet-Saguy had a grant from the Marie-Curie contract N. HPMF 2001- 00389 "European Doctoral School on Structural Biology".

Supporting Information Available: Table S1 and ^{1}H, ^{15}N, and ^{13}C NMR data for iron(III) holoHasAwt in $^{1}H_2O$, 20 mM phosphate, pH 5.6, at 303 K. This material is available free of charge via the Internet at http://pubs.acs.org.

JA054902H

(67) Bertini, I. F., I. C.; Kümmerle, R.; Moskau, D.; Pierattelli R. *J. Am. Chem. Soc.* **2004**, *126*, 464−465.

(68) Letoffe, S.; Delepelaire, P.; Wandersman, C. *J. Bacteriol.* **2004**, *186*, 4067−4074.